NANO LETTERS

2007
Vol. 7, No. 11
3388−3393

Hierarchical Silicon Etched Structures for Controlled Hydrophobicity/ Superhydrophobicity

Yonghao Xiu,[†,‡] Lingbo Zhu,[†,‡] Dennis W. Hess,*[,†] and C. P. Wong*[,‡]

School of Chemical and Biomolecular Engineering, Georgia Institute of Technology, 311 Ferst Drive, Atlanta, Georgia 30332-0100, and School of Materials Science and Engineering, Georgia Institute of Technology, 771 Ferst Drive, Atlanta, Georgia 30332-0245

Received July 18, 2007; Revised Manuscript Received September 3, 2007

ABSTRACT

Silicon surface hydrophobicity has been varied by using silane treatments on silicon pyramid surfaces generated by KOH anisotropic etching. Results demonstrated that by altering the surface hydrophobicity, the apparent contact angle changed in accord with the Wenzel equation for surface structures with inclined side walls. Hierarchical structures were also constructed from Si pyramids where nanostructures were added by Au-assisted electroless HF/H_2O_2 etching. Surface hydrophobicity and superhydrophobicity were achieved by surface modification with a variety of silanes. Stability of the Cassie state of superhydrophobicity is described with respect to the Laplace pressure as indicated by the water droplet meniscus in contact with the hierarchical structures. The contact angle hysteresis observed is also discussed with respect to water/substrate adhesion.

The effect of surface structure on superhydrophobicity is of much interest due to the dependence of structure on the attainment of a high-water contact angle (>150°) and reduced contact angle hysteresis (<10°). Superhydrophobicity was first observed on lotus leaves where high-water contact angle and low hysteresis cause water that falls on the surface to bead and roll off the surface, thereby leading to water repellency and self-cleaning characteristics.[1−3] Such surface properties are also critical in microelectromechanical systems (MEMS) antistiction,[4] friction reduction,[5] and anticorrosion[6] applications. In addition, superhydrophobic surfaces offer much promise for the formation of high-performance micro-/nano-structured surfaces with multifunctionality that can be used in optical,[7,8] photoelectric,[9] microelectronic, catalytic, and biomedical applications.

In many instances, superhydrophobicity is achieved on a hierarchically structured surface. For instance, although both the Wenzel state and the Cassie state display a high-contact angle, a Cassie state is required for reduced adhesion. To achieve the Cassie state, the Young's contact angle on a surface must be greater than a critical contact angle θ_c.[10] Substantial effort has been expended on the generation of micron-scale-structured surfaces that also possess nanoscale roughness.[11−15] However, most of the micron-scale structures reported are structures with vertical walls;[13,14] generally, these structures alone can maintain a Cassie state. Although the Cassie state does not ensure superhydrophobicity, addition of nanoscale roughness can facilitate attainment of superhydrophobicity. For micron-scale structures in the Wenzel state, the ability to achieve superhydrophobicity is even more limited. That is, for a surface in the Wenzel state to be converted into a Cassie state, nanoscale structures are needed even after a hydrophobic surface treatment. The effect of roughness on superhydrophobicity can be shown clearly from the Wenzel and Cassie−Baxter equations. However, the detailed effect of hierarchical structure on the Laplace pressure (as indicated by the water meniscus) and thus on the work of adhesion is not delineated by these two equations. Because the Laplace pressure establishes the contact angle and contact angle hysteresis, it is important to investigate the effect of surface structure on the Laplace pressure. Lafuma et al. have demonstrated that the Cassie to Wenzel transition can be induced by applying a pressure on the water droplet.[10] In addition, Bormashenko et al. recently demonstrated that the transition can also be induced by vertical vibration of a water droplet on rough surfaces.[16]

In this study, we mimick the hierarchical structure of lotus leaves by preparing an artificial superhydrophobic surface by simple silicon-etching techniques to demonstrate the effect of two scale roughness on superhydrophobicity. Micron-scale pyramid structures were generated by anisotropic KOH etching; the nanostructures were prepared by metal-assisted

* Corresponding authors. (D.W.H.) Tel: 1-404-894-5922. Fax: 1-404-894-2866. E-mail: dennis.hess@chbe.gatech.edu. (C.P.W.) Tel: 1-404-894-8391. Fax: 1-404-894-9140. E-mail: cp.wong@mse.gatech.edu..

† School of Chemical and Biomolecular Engineering.

‡ School of Materials Science and Engineering.

10.1021/nl0717457 CCC: $37.00
Published on Web 10/11/2007

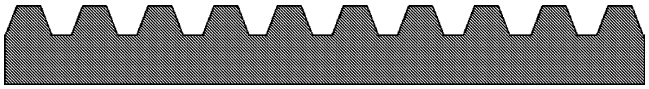

Figure 1. Model structure of inclined side walls on a substrate surface.

HF/H_2O_2 etching.[7,9,17] The ability to transform a surface from a Wenzel state to a Cassie state that displays superhydrophobicity was demonstrated by controlling the surface structures and surface hydrophobicity.

Experimental Details. n-type silicon (100) wafers with a resistivity of 3−10 Ω cm were used in all experiments. KOH etching was performed in a solution of KOH (3 wt %), water, and isopropyl alcohol (20% by volume) at 85 °C for 20−30 min. Prior to metal assisted etching, a thin discontinuous layer of Au with a thickness of 5 nm was deposited by e-beam evaporation. Etching was then performed for various times in a HF/H_2O_2 solution (49% HF, 30% H_2O_2, and H_2O with a volume ratio of 1:5:10). Subsequently, the Au nanoparticles of diameter ∼5−10 nm were removed by immersing the samples in KI/I_2 (100 g KI and 25 g I_2 per 1L H_2O) for 60 s.

Contact angle measurements were performed with a Rame−Hart goniometer that had a charge-coupled device camera equipped for image capture. Scanning electron microscopy (SEM) was used to investigate the surface morphology. After fabrication of the surface structure, surface fluorination was performed by treatment with various fluoroalkylsilanes. Ten millimolar solutions of 3,3,3-trifluoropropyl-trichlorosilane (TFPS), dodecyltrichlorosilane (DTS), octadecyltrichlorosilane (ODTS), and perfluorooctyl trichlorosilane (PFOS) were dissolved in hexane. For a specific treatment, the structured silicon wafer was immersed in one of these solutions for 30 min followed by a heat treatment at 150 °C in air for 1 h, to complete the hydrophobic surface modification.

Results and Discussion. When surfaces are randomly roughened, the surface structures are not vertically oriented to the substrate; thus, they often show inclined walls as shown schematically in Figure 1. The contact angle dependence on the wall angles of such surface structures is important when superhydrophobicity is desired. The studies described below have generated silicon pyramids to serve as a model surface for the investigation of the effect of inclined (nonperpendicular) side-wall angles on hydrophobic and superhydrophobic behavior. Micron-sized surface pyramids were prepared by anisotropic KOH etching of silicon substrates with (100) orientation; the bases on these pyramids result from the intersection of (111)-orientated crystallographic planes. An SEM image of the surface is shown in Figure 2a. This surface was treated with PFOS which yielded a contact angle of 146.3° and a contact angle hysteresis >60°. Deposition of nanometer-sized Au particles on this pyramidal surface was followed by silicon etching in HF/H_2O_2 for 60 s and then removal of the Au nanoparticles in KI/I_2 for 60 s. These treatments resulted in the production of surface nanostructures directly on the pyramid surfaces. After PFOS treatment, the surface displayed superhydrophobicity with a contact angle as high as 165.8° and small (<5°) contact angle hysteresis.

Superhydrophobicity is usually achieved through the formation of a composite interface (solid/water and air/water interfaces) with air trapped within the structure.[18] Figure 3 illustrates the geometry involved when water contacts surface structures with inclined walls. The Laplace pressure as indicated by the meniscus at the water droplet/surface contact, plays an important role in maintaining a composite interface by confining the water at the air/water interface. According to previous studies that investigated the effect of inclined walls on the Laplace pressure,[19] for two inclined walls as shown in Figure 3 the relationship between the Laplace pressure and the inclination angle α can be described by eq 1 as

$$\Delta p = p - p_0 = -\frac{\gamma \cos(\theta - \alpha)}{R_0 + h \tan \alpha} \tag{1}$$

where γ is the surface tension of water, θ is Young's contact angle of liquid on the surface, α is the inclination angle as illustrated in Figure 3, R_0 is half of the width between base edges of two adjacent inclined walls, p is the pressure on the liquid side of the meniscus, and p_0 is atmospheric pressure. Equation 1 is analogous to the Laplace equation if written in the form $\Delta p = c\gamma \cos \theta / r$, where the contact angle is $\theta - \alpha$ and r is $R_0 + h \tan \alpha$ (the constant c is $c = 1$ for two parallel and flat surfaces separated at distance $2r$, or $c = 2$ for cylindrical capillary in which r is the radius of capillary). From eq 1, it is clear that the Laplace pressure is dependent on the surface tension of water γ, height h, width R_0, Young's contact angle θ, and inclination angle α. The height h is dependent upon the hydrostatic pressure of water on top of the structured surface. For two vertical and parallel walls separated at distance $2R_0$, α is 0°, $r = R_0$, and the Laplace equation is reduced to

$$\Delta p = -\frac{\gamma \cos \theta}{R_0} \tag{2}$$

Equation 1 indicates that the Laplace pressure is reduced due to the side wall (surface) inclination angle α; the higher the inclination angle, the more reduction in the Laplace pressure. When the inclination angle is sufficiently high for a particular surface structure (depending on θ), there is no air entrapment, and water wets the structured surface completely. In a metastable Cassie state, application of pressure to the water droplet can affect the hysteresis if the drop adheres to the surface, thereby leading to a transition from a Cassie state to a Wenzel state. The transition pressure is related to the Laplace pressure that confines the droplet to the composite surface. For a structured surface with an inclination angle, the transition takes place at a lower pressure.

A schematic illustrating the range of possible wetting scenarios with varying inclination angles is illustrated in Figure 4. Equation 1 indicates that inclined surfaces can inhibit achievement of a superhydrophobic state relative to

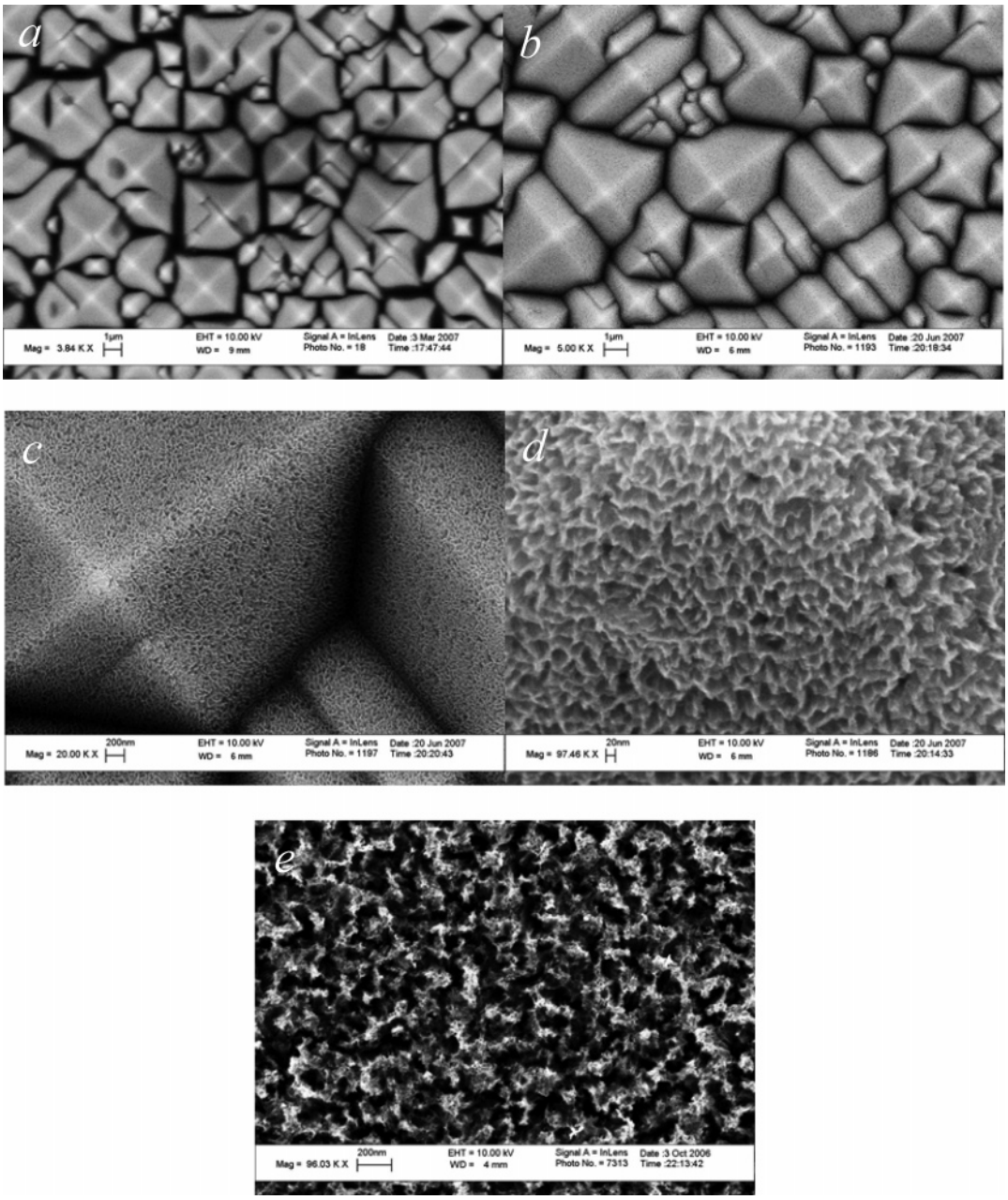

Figure 2. Silicon surface structures after etching in KOH at 80 °C for 25 min (a), two scale rough surfaces resulting from pyramid + nanostructure from Au-assisted HF/H_2O_2 etching; different magnifications (b,c,d) and nanostructures on a flat silicon surface with (111) orientation (e) from Au assisted etching are shown.

the situation observed with vertical structures. Interestingly, this scenario is the one that is most likely encountered in nature. For structures with vertical walls, the water meniscus either remains on top of the structure or moves to the bottom of the structure when pressure is applied to the water droplet. However, as a result of the inclination angle (eq 1), the Laplace pressure increases when the meniscus approaches the structure bottom (decreasing h, as shown in Figure 3). Equation 1 also indicates that when the surface hydrophobicity increases (increase of θ), the Laplace pressure increases and more air can be trapped between the structures, leading to an increase in apparent contact angle and reduced contact angle hysteresis (reduced contact area) as illustrated in Figure 4.

The dependence of the apparent contact angle on Young's contact angle and surface roughness is shown in Figure 5 as calculated from the Wenzel and Cassie−Baxter equations. For the Cassie state, the surface solid/liquid contact fraction f_1 is critical to establishing the apparent contact angle, while Young's contact angle is not an important factor. However, the Wenzel state is more dependent on Young's contact angle. That is, surface hydrophobicity can be used to effectively increase the apparent contact angle for Wenzel states, while for Cassie states, a reduction of the fraction of solid/water contact is more effective.

For silicon surfaces with micron-sized pyramids, the effect of surface hydrophobicity on contact angle was investigated by performing surface treatments with a variety of different

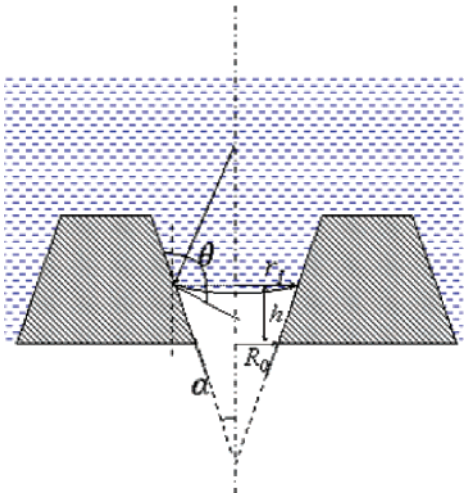

Figure 3. Water contact at surface structures with inclined walls.

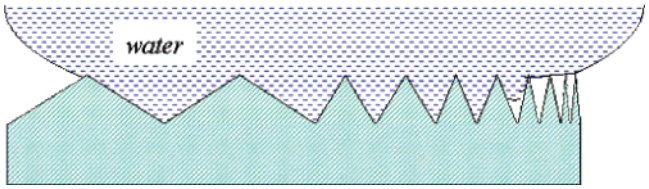

Figure 4. Water droplet on a hydrophobic surface with inclined wall structures of various angles.

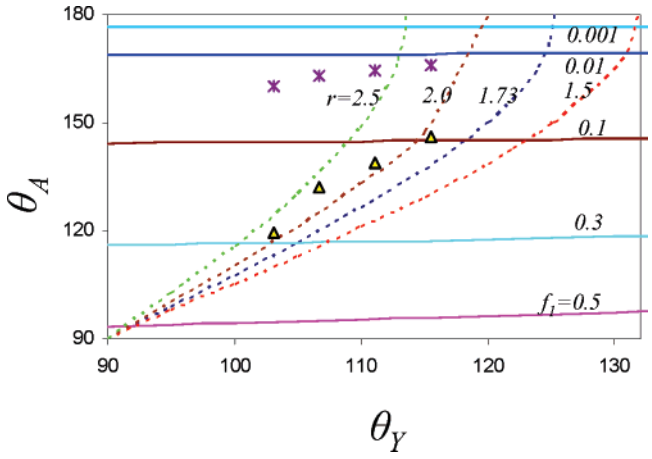

Figure 5. Contact angle calculations based on the Wenzel equation: $\cos\theta_A = r\cos\theta_Y$ (dotted lines) and on the Cassie–Baxter equation: $\cos\theta_A = f_1\cos\theta_Y + f_1 - 1$ (solid lines). Data points: stars represent the contact angles on two-scale rough silicon surfaces; triangles represent the contact angles on micron-scale pyramid surfaces; both surfaces have undergone silane treatments as described in Table 1.

silanes that display different Young's contact angles on the surface (Table 1).

The triangles in Figure 5 designate the contact angles observed after silicon pyramid surfaces were treated with the four different silanes listed in Table 1. With an increase in surface hydrophobicity (Young's contact angle), the apparent contact angles increase, consistent with the Wenzel equation. According to the data in Figure 5, the Wenzel surface roughness factor is ~2.0. Previous studies[20] have suggested that for surface structures with inclined side walls,

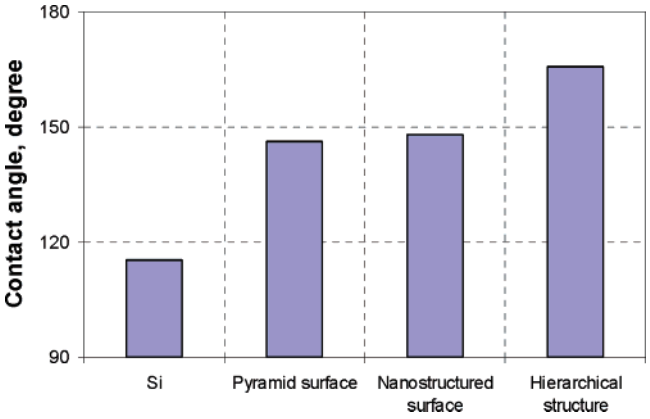

Figure 6. Contact angles on silicon surfaces with different surface texturing after PFOS treatment. For a silicon pyramid surface that possesses a hierarchical structure, a superhydrophobic surface with minimum hysteresis results after PFOS treatment. Nanostructures have been formed by Au-assisted etching of silicon surfaces in HF/H_2O_2 for 60 s with a Au layer of 5 nm on the silicon (111) surface.

there is no energy barrier for the transition between the Wenzel state and Cassie state if Young's contact angle $\theta_Y < 90° + \alpha$. Therefore, the Cassie state will always transition to the Wenzel state because it is a lower energy state. Indeed, our observations indicate that although the contact angle is higher (Cassie state) when the water droplet initially touches the pyramid surface, the contact angle drops quickly to a lower value (Wenzel state) as a result of the absence of an energy barrier between the two states.

An effective way to increase the Laplace pressure for superhydrophobicity is to generate nanostructures on the silicon pyramid surface, as shown in Figure 6; SEM images of the surface hierarchical structures are shown in Figure 2b,c,d. For a surface with inclined wall structures, the wetting behavior represents a combination of air entrapment, surface hydrophobicity, and wall inclination. For two-scale structures on silicon surfaces, we presume that the nanostructure, as shown in Figure 2d, merely improves the surface hydrophobicity because the contact angle after PFOS treatment is 148.1°; this contact angle was obtained on nanostructures from Au-assisted etching of a Si(111) surface, as shown in Figure 2e. However, if the surface has only micron-scale pyramids with a Young's surface contact angle of ~115° after PFOS treatment, the surface is not superhydrophobic. According to eq 1, the Laplace pressure is greatly enhanced when a high contact angle θ exists. In addition, the extended three phase contact line on smooth surfaces is segmented into smaller contact lines on pyramidal surfaces with nanostructures. As a result, the surface exists in a stable Cassie state and is superhydrophobic. This leads to an improvement in the superhydrophobic stability on micron-scale pyramid surfaces with air entrapment at the composite contact interface. The result of forming a hierarchical structure is to achieve/enhance the Cassie state and thus the surface superhydrophobicity through the interplay of surface hydrophobicity, air entrapment, and inclination angle. Such effects cannot be achieved readily by structures with only one size scale. On two-scale rough surfaces, an increase of surface hydrophobicity also improves the apparent contact

Table 1. Contact Angles Resulting from Different Silane Treatments

silane	sessile drop contact angles on a flat Si surface (degree)	sessile drop contact angles on a silicon pyramid surface (degree)	advancing contact angles on a two scale structured Si surface (degree)	contact angle hysteresis (degree)
TFPS	103.1	119.7	160.2	28.2
DTS	106.7	132.1	162.9	17.9
ODTS	111.0	139.1	164.7	4.4
PFOS	115.5	146.3	165.8	2.1

Table 2. Contact Angle Hysteresis on Different Textured Surfaces after PFOS Treatment

surfaces	hysteresis
Si	
silicon pyramids	>60°
silicon nanostructured surface[a]	>60°
hierarchically structured pyramid surface[a]	2.1°

[a] Nanostructures formed from Au-assisted etching of silicon surfaces in HF/H_2O_2 for 60 s with Au layer of 5 nm on the silicon (111) surface.

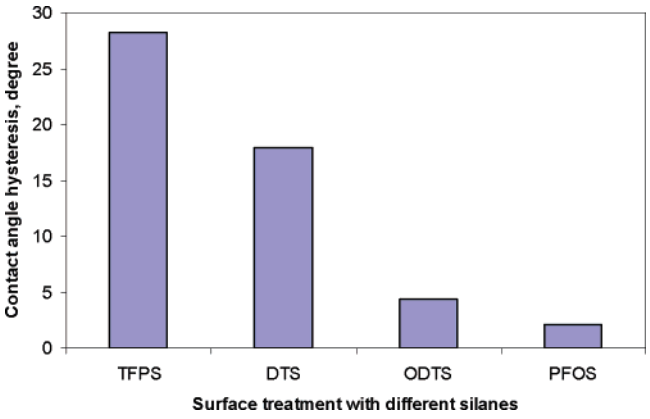

Figure 7. Hysteresis on two-scale structured surfaces with different silane treatments.

angle, but the effect is not large, because these surfaces already show very high contact angles in the Cassie state as shown in Table 1 and Figure 3 (stars).

The hierarchical structures not only facilitate improvement of the apparent contact angle but also reduce the contact angle hysteresis as shown in Table 2.

For contact angle hysteresis related to water/solid adhesion, the hydrophobic surface plays two roles. First, adhesion of the solid/water contact interface is reduced due to the lowered surface tension of the solid surface γ_s; the work of adhesion can be estimated as $w_{ad} = 2\sqrt{\gamma_w \gamma_s}$.[21] Second, the increased hydrophobicity of the surface gives a higher water contact angle (θ) on the surface due to the change in surface free energy. This results in a higher Laplace pressure, and so the meniscus moves away from the bottom of the structures. Therefore, the water/solid contact area is reduced leading to reduced adhesion between water and the solid surface. This fact is manifested in a difference in contact angle hysteresis of two-scale rough surfaces that have different silane treatments as shown in Figure 7. Such observations also confirm the proposal that hysteresis is more important than contact angle in achieving superhydrophobicity.[22]

Conclusion. Surface structures with inclined wall angles play an important role in establishing superhydrophobicity because they inhibit the ability to achieve a stable Cassie state. This consideration is related to the Laplace pressure at the water meniscus, which helps to maintain a composite contact interface. Surface hydrophobicity was varied by using different silane treatments on silicon pyramid surfaces to demonstrate that for these structured surfaces, the stable state is the Wenzel state. By changing the surface hydrophobicity, the apparent contact angle changes according to the Wenzel equation for surface structures with inclined side walls, where the surface roughness and Young's contact angle establish the apparent contact angles. Superhydrophobicity can only be achieved if a second scale nano rough surface is constructed on top of the silicon pyramid surface to maintain a stable Cassie state. With such structures, the apparent contact angles are dependent on the contact fraction of solid/water, while Young's contact angle plays a less important role. The surface liquid/solid contact area, hydrophobicity, and geometry of surface structures are thus interrelated in establishing superhydrophobicity. An increase in the surface hydrophobicity (Young's contact angle) leads to a decrease in the water/substrate contact area fraction and therefore a reduction in contact angle hysteresis and an increase in the apparent contact angle. These studies offer additional approaches for the design of surface structures with geometries appropriate for the attainment of superhydrophobicity and stability; the ability to tailor surfaces for specific properties, for example, optical, electrical, biomedical, may also be facilitated. On randomly roughened surfaces, the inclination angles display a distribution. We expect that at low-surface hydrophobicity, only structures with small inclination angles trap air to form air cushions/composite interfaces. As the surface hydrophobicity increases, structures with large inclination angles begin to trap air, thereby leading to a reduced water/surface contact area. This may help to explain the observation from Lafuma et al. that the transition pressure from Cassie state to Wenzel state is much lower than the Laplace pressure needed for water to penetrate the surface structure.[10]

Acknowledgment. The authors would like to acknowledge financial support from the National Science Foundation (NSF CMMI No. 0621115) and the National Electric Energy Testing Research and Applications Center (NEETRAC) at Georgia Institute of Technology.

References

(1) Neinhuis, C.; Barthlott, W. Characterization and distribution of water-repellent, self-cleaning plant surfaces. *Ann. Bot.* **1997**, *79* (6), 667−677.

(2) Barthlott, W.; Neinhuis, C. Purity of the sacred lotus, or escape from contamination in biological surfaces. *Planta* **1997**, *202* (1), 1−8.

(3) Neinhuis, C.; Koch, K.; Barthlott, W. Movement and regeneration of epicuticular waxes through plant cuticles. *Planta* **2001**, *213* (3), 427−434.

(4) Bhushan, B.; Jung, Y. C. Micro- and nanoscale characterization of hydrophobic and hydrophilic leaf surfaces. *Nanotechnology* **2006**, *17* (11), 2758−2772.

(5) Cottin-Bizonne, C.; Barrat, J.-L.; Bocquet, L.; Charlaix, E. Low-friction, flows of liquid at nanopatterned interfaces. *Nat. Mater.* **2003**, *2* (4), 237−240.

(6) Wang, S. T.; Feng, L.; Jiang, L. One-step solution-immersion process for the fabrication of stable bionic superhydrophobic surfaces. *Adv. Mater.* **2006**, 18 (6), 767-+.

(7) Chattopadhyay, S.; Li, X. L.; Bohn, P. W. In-plane control of morphology and tunable photoluminescence in porous silicon produced by metal-assisted electroless chemical etching. *J. Appl. Phys.* **2002**, *91* (9), 6134−6140.

(8) Campbell, P.; Green, M. A. Light Trapping Properties of Pyramidally Textured Surfaces. *J. Appl. Phys.* **1987**, *62* (1), 243−249.

(9) Koynov, S.; Brandt, M. S. Stutzmann, M. Black nonreflecting silicon surfaces for solar cells. *Appl. Phys. Lett.* **2006**, 88 (20), 203107-1−203107-3.

(10) Lafuma, A.; Quere, D. Superhydrophobic states. *Nat. Mater.* **2003**, *2* (7), 457−460.

(11) Xiu, Y.; Zhu, L.; Hess, D. W.; Wong, C. P. Biomimetic creation of hierarchical surface structures by combining colloidal self-assembly and Au sputter deposition. *Langmuir* **2006**, *22* (23), 9676−9681.

(12) Gao, X. F.; Yao, X.; Jiang, L. Effects of rugged nanoprotrusions on the surface hydrophobicity and water adhesion of anisotropic micropatterns. *Langmuir* **2007**, *23* (9), 4886−4891.

(13) Gao, L. C.; McCarthy, T. J. The "lotus effect" explained: Two reasons why two length scales of topography are important. *Langmuir* **2006**, *22* (7), 2966−2967.

(14) Zhu, L.; Xiu, Y.; Xu, J. W.; Tamirisa, P. A.; Hess, D. W.; Wong, C. P. Superhydrophobicity on two-tier rough surfaces fabricated by controlled growth of aligned carbon nanotube arrays coated with fluorocarbon. *Langmuir* **2005**, *21* (24), 11208−11212.

(15) Zheng, Y. M.; Gao, X. F.; Jiang, L. Directional adhesion of superhydrophobic butterfly wings. *Soft Matter* **2007**, *3* (2), 178−182.

(16) Bormashenko, E.; Pogreb, R.; Whyman, G.; Erlich, M. Cassie-Wenzel Wetting Transition in Vibrating Drops Deposited on Rough Surfaces: Is the Dynamic Cassie-Wenzel Wetting Transition a 2D or 1D Affair? *Langmuir* **2007**, 23, 6501−6503.

(17) Li, X.; Bohn, P. W. Metal-assisted chemical etching in HF/H2O2 produces porous silicon. *Appl. Phys. Lett.* **2000**, *77* (16), 2572−2574.

(18) Patankar, N. A. On the modeling of hydrophobic contact angles on rough surfaces. *Langmuir* **2003**, *19* (4), 1249−1253.

(19) Tsori, Y. Discontinuous liquid rise in capillaries with varying cross-sections. *Langmuir* **2006**, *22* (21), 8860−8863.

(20) Patankar, N. A. Transition between superhydrophobic states on rough surfaces. *Langmuir* **2004**, *20* (17), 7097−7102.

(21) Israelachvili, J. *Intermolecular and surface forces*, 2nd ed.; Academic Press: 1991; p 450.

(22) Chen, W.; Fadeev, A. Y.; Hsieh, M. C.; Oener, D.; Youngblood, J.; McCarthy, T. J. Ultrahydrophobic and Ultralyophobic Surfaces: Some Comments and Examples. *Langmuir* **1999**, *15* (10), 3395−3399.

NL0717457